A Compact Broadband Dual Polarized Patch Antenna for Satellite Communication/Navigation Applications

Jiang Long, *Student Member, IEEE,* and Daniel F. Sievenpiper, *Fellow, IEEE*

***Abstract*—In this letter, a compact and robust dual circularly polarized patch antenna for combined Globalstar/GPS application has been presented. The designed patch antenna is accomplished with size of $40 \times 40 \times 6$ mm^3 over the frequency bandwidth of 1570–1650 MHz, which is $0.21\lambda_0 \times 0.21\lambda_0 \times 0.03\lambda_0$ (λ_0 is the free space wavelength at the lowest frequency of the operating bandwidth). Instead of air substrate, high permittivity substrate is adopted for the size reduction. The bandwidth reduction due to the inclusion of the high permittivity substrate is compensated by introducing a parasitic patch. In addition, a 90° hybrid is utilized for achieving dual circular polarization. The designed antenna is validated by the measurement, presenting a 5% fractional bandwidth (1570–1650 MHz) for both VSWR < 2, axial ratio less than 3 dB, and port isolation less than -6 dB.**

***Index Terms*—Dual circular polarization, patch antenna, broadband antenna, parasitic patch.**

I. Introduction

NOWADAYS, satellite communication systems (1610–1626.5 MHz), such as Globalstar, usually incorporate global navigation satellite systems (most operating at L1 band: 1575.4 ± 10.23 MHz, and L2 band: 1227.6 ± 10.23 MHz), such as American GPS, so as to simultaneously provide location/time information as well as data/voice services, which has greatly facilitated various applications for all civil, commercial, and military purposes. Consequently, two requirements are imposed to the antennas for such combined satellite communication/navigation system. Firstly, since Globalstar requires left hand circular polarization (LHCP), whereas GPS system uses right hand circular polarization (RHCP), the antennas are supposed to be dual circularly polarized (CP). Secondly, despite of the closely allocated operating frequency bands, the antenna should cover at least 1565–1626 MHz, a 4% fractional bandwidth, which is still a challenge for small antenna design. Due to all these considerations, many patch antennas have been reported with thick air-substrates [1]–[5] and alternative feeding techniques [4], [5] for covering the required bandwidth. Also, single patch with dual feeds [4] and multiple patches with a shared feed [6] can be applied for achieving dual CP.

In addition to the aforementioned two requirements on the bandwidth and polarization, compactness and robustness are increasingly demanding owning to the mobility of various applications. Therefore, in this letter, we present a compact and robust dual CP patch antenna for combined Globalstar/GPS applications. Instead of using an air substrate, the antenna is designed with a high permittivity substrate for achieving robustness and size reduction. Additional slots are also adopted, so that the patch can reside in a total size as small as $40 \times 40 \times 6$ mm^3. Since the inclusion of the high permittivity substrate inevitably reduces the bandwidth and efficiency [7]–[9], a parasitic patch is employed for increasing the bandwidth to meet the requirement of the Globalstar and GPS application. A compact 90° hybrid is utilized for generating a quadrature feed to the antenna. RHCP and LHCP are achieved at the two isolated ports of the hybrid. The fabricated antenna has

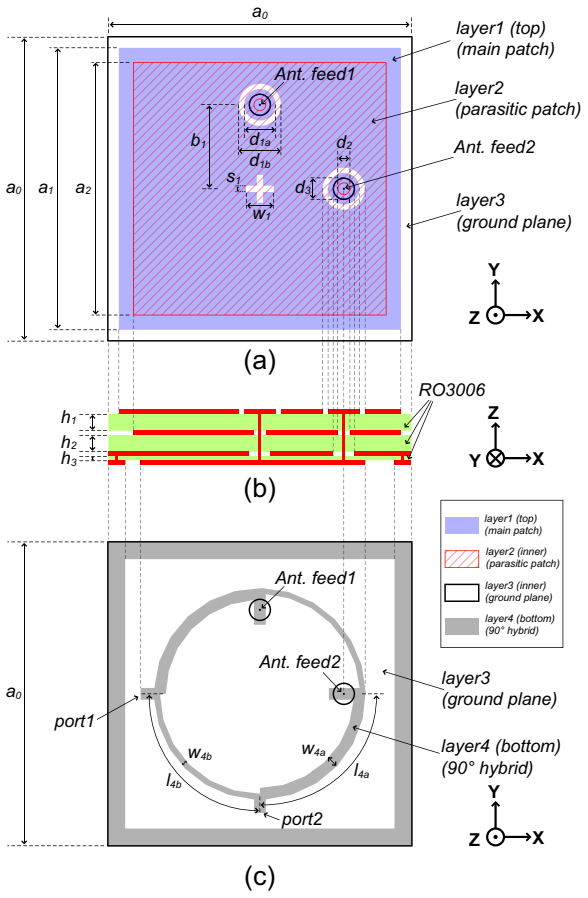

Fig. 1. The geometry of the designed antenna. (a) First three layers from top, for radiating patches. (b) Stack-up illustration. (c) Last two layers from the bottom, for feeding network.

Manuscript received July 12, 2014, revised Sep. 14, 2014. This work was supported by SPAWAR.

J. Long and D. F. Sievenpiper are with the Department of Electrical and Computer Engineering, University of California, San Diego, La Jolla, 92093 USA e-mail: jilong@ucsd.edu, dsievenpiper@eng.ucsd.edu.

TABLE I
DIMENSIONS FOR THE ANTENNA

Dimensions	a_0	a_1	a_2	d_{1a}	d_{1b}	s_1
(mm)	40	36.83	35.3	4.98	4.57	3.68
Dimensions	w_1	b_1	d_2	d_3	l_{4a}	w_{4a}
(mm)	0.76	11.5	1.52	3	21.94	1.62
Dimensions	l_{4b}	w_{4b}	h_1	h_2	h_3	
(mm)	22.65	0.9	2.54	2.54	0.65	

been measured, showing a 5% fractional bandwidth (1570–1650 MHz) for both VSWR < 2, axial ratio (AR) less than 3 dB, and port isolation less than -6 dB. The measured antenna efficiency is above 70% over the bandwidth of interest. The accomplished antenna can be used for both Globalstar and GPS applications.

II. ANTENNA STRUCTURE AND DESIGN

The antenna to be designed are intended to be compact (limited to 40×40 mm^2 area, and as thin as possible), robust, dual CP, stable over the bandwidth of 1565–1626 MHz, and as simple as possible. Therefore, a patch antenna with quadrature feeds has been adopted. Instead of using an air substrate, high permittivity substrate (RO3006, $\epsilon_r = 6.5$) is used for reducing the antenna size. The loss of the substrate material, $tan\delta = 0.002$, is considered in this design. In addition, the adoption of the solid substrate material without an air gap between the patch and the ground plane enhances the robustness of the antenna, and additionally simplifies the fabrication to printed circuit board (PCB) process. The antenna structure and dimensions are illustrated in Fig. 1.

The final size of the antenna is confined to $40 \times 40 \times 6$ mm^3. It consists of four layers. The top layer is a square patch ($a_1 \times a_1$) with two crossing rectangular slots ($w_1 \times s_1$) and two circular holes (d_{1b}) which are located with an offset of b_1 from the center, where two feeding pads (d_{1a}) are placed. The second layer is a parasitic square patch ($a_2 \times a_2$) for enhancing the bandwidth. It is isolated from the feed with a hole (d_2). The third layer is the ground with the same size as the whole substrate ($a_0 \times a_0$). The clearance to the feed on this layer is d_3. A 90° hybrid and a grounded ring are printed on the bottom layer. All the dimensions are listed in table I.

As the main radiator, the patch and the slots are optimized to resonate at 1600 MHz. A capacitive feeding structure is utilized for increasing the matching bandwidth. The position of the feed is also optimized in the simulation for achieving the best input impedance matching.

For the sake of CP, a quadrature feed configuration is adopted. A 90° hybrid is implemented in a circular shape and placed under the ground plane. It is composed of four quarter-wavelength transmission lines with characteristic impedance of 50 Ω and 35.4 Ω [10]. The circuit model of the hybrid, the designed microstrip structure, and its simulated performance are presented in Fig. 2, which indicates perfect matching for the input port of the hybrid (i.e., P1 and P4) and 90° phase difference between the two outputs that connected to the antenna (i.e., $\phi_{P2} - \phi_{P3}$). It thus can be seen that when

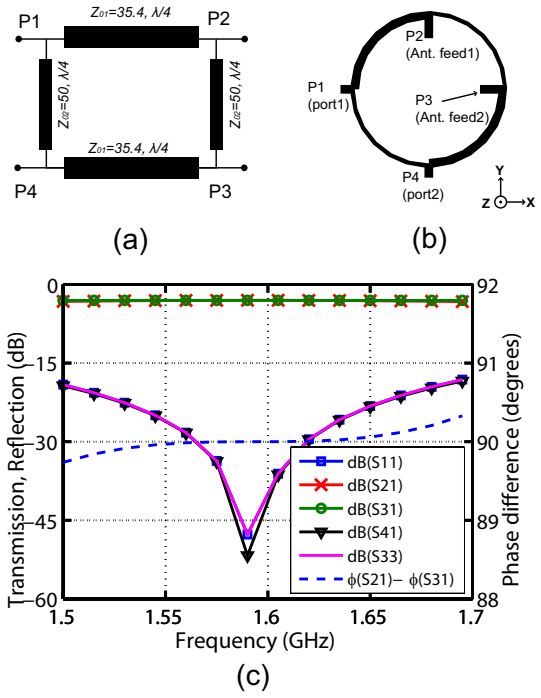

Fig. 2. The designed 90° hybrid. (a) the circuit model; (b) the designed microstrip layout; (c) the simulated performance.

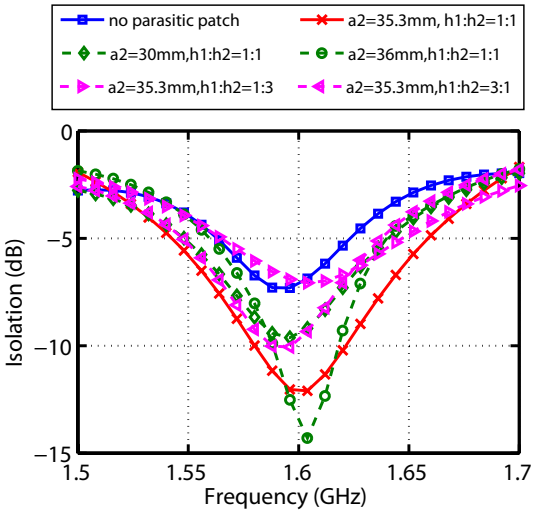

Fig. 3. Simulated port isolation with and without the parasitic patch and its parametric study.

the feeding network is excited at P1 (port-1), P2 (antenna feed-1) and P3 (antenna feed-2) have the relative phase of 90° and 0°, respectively, which results in LHCP. By contrast, RHCP can be obtained by exciting the hybrid at P4 (port-2).

Since the high permittivity substrate ($\epsilon_r = 6.5$) is involved and the fact that the size of the antenna is extremely confined in the limited space, in particular, due to the thin substrate thickness, which is only 6 mm, about $0.03\lambda_0$, the radiating patch (top layer) itself does not provide satisfactory bandwidth [7]–[9]. Consequently, with the hybrid, such imperfect matching results in undesirable isolation of the two input ports (i.e., P1 and P4). Therefore, a parasitic patch is added for

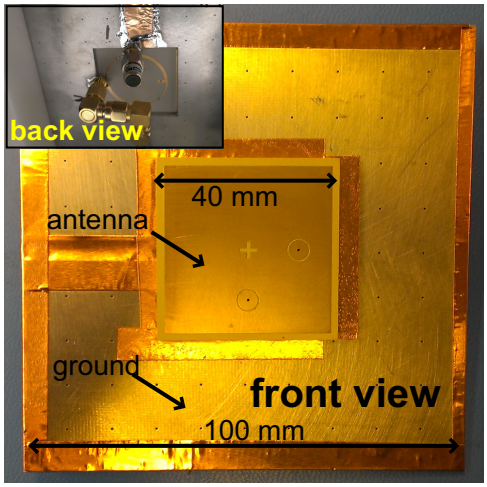

Fig. 4. The fabricated antenna mounted on a 100 mm ground.

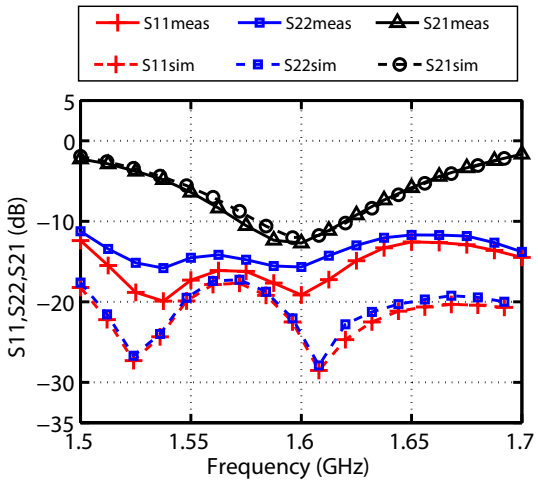

Fig. 5. The measured input impedance matching at port1 and port2, and the port isolation.

increasing the impedance matching bandwidth of the top patch, so that the isolation can be improved. The parametric study on the patch size (a_2) is presented in Fig. 3. It can be seen that when $a_2 = 30$ mm the isolation is almost the same as the case without the parasitic patch. The isolation improves when a_2 increases to 35.3 mm or even more, whereas the isolation bandwidth decreases. Therefore, owning to this trade-off between the isolation and the bandwidth, $a_2 = 35.3$ mm is taken so that the isolation less than -6 dB over the bandwidth of 1550–1650 MHz is achieved. The ratio of h_1 to h_2 is also investigated (the total thickness is kept as 5.08 mm, i.e., $h_1 + h_2 = 5.08$ mm), and shown in Fig. 3, from which it is found that the isolation degrades when the parasitic patch is closed to either top patch or the ground plane. Thus, h_1 and h_2 are chosen to be equal. This is also good for substrate material selection.

III. Fabrication and Measurement

The fabricated antenna is shown in Fig. 4, where the antenna block is mounted on a 100×100 mm^2 square ground plane.

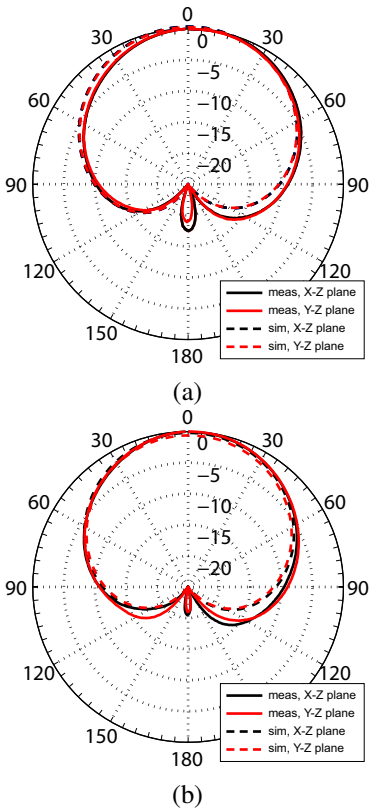

Fig. 6. Simulated and measured gain pattern of the principle polarization (LHCP), when excitation is at port-1. (a)1575 MHz; (b)1621 MHz.

The inset figure illustrates the back view of the fabricated antenna, which reveals that two SMAs are directly soldered to the input port of the 90° hybrid for providing microstrip to coax transition. From the front view, the antenna is mounted to the ground plane through adhesive and conductive cooper tape. Instead of soldering the ground plane and the antenna together, adhesive cooper tape is utilized for fabrication because of simplicity, which, however, does introduce extra loss, but can still demonstrate the functionality of the proposed antenna.

The simulated and measured impedance matching at the two input ports and their isolation are presented in Fig. 5. It can be seen that -10 dB impedance matching is achieved over the bandwidth of 1500–1700 MHz, and -6 dB isolation is accomplished from 1550 MHz to 1650 MHz. The good coherence of the simulated and measured impedance matching performance validates the fabricated antenna.

The normalized gain patterns of the antenna for both x-z and y-z planes are measured and plotted in Fig. 6 for 1575 MHZ and 1621 MHz with excitation at port-1, and in Fig. 7 for port-2 excited. For pattern excited at port-1, LHCP is the principle polarization, whereas, RHCP corresponds to the pattern excited by port-2. The almost identical patterns for x-z and y-z plane indicate the property of axial symmetry. The great agreement of the measurement and simulation validates the design.

Fig. 8 shows the peak gains for the principle polarizations and the ARs in the direction of maximum radiation (z-axis). The ARs for both excitations are below 3 dB over the

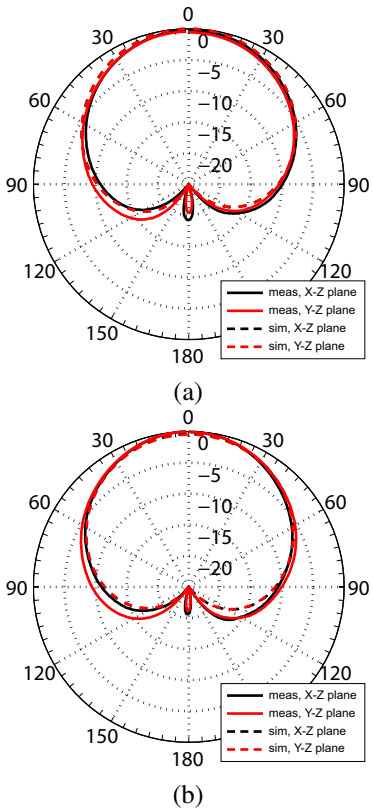

Fig. 7. Simulated and measured gain pattern of the principle polarization (RHCP), when excitation is at port-2. (a)1575 MHz; (b)1621 MHz.

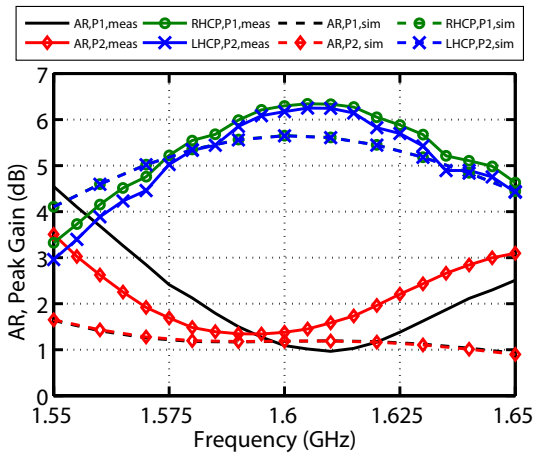

Fig. 8. Simulated and measured peak gain and AR in z-direction.

bandwidth of 1570–1650 MHz. The peak gain is above 5 dBi from 1565 MHz to 1630 MHz. The peak gain also exhibits its maximum at 1600 MHz, and decreases toward both higher and lower frequencies, which is due to the imperfect port isolation. The simulated and measured antenna efficiencies are presented in Fig. 9, showing over 70% efficiency for the bandwidth of 1570–1630 MHz. The rolling off of the efficiency from 1.6 GHz is also because of the -6 dB port isolation. The measured results show the antenna can be used for both GPS and Globalstar appliations.

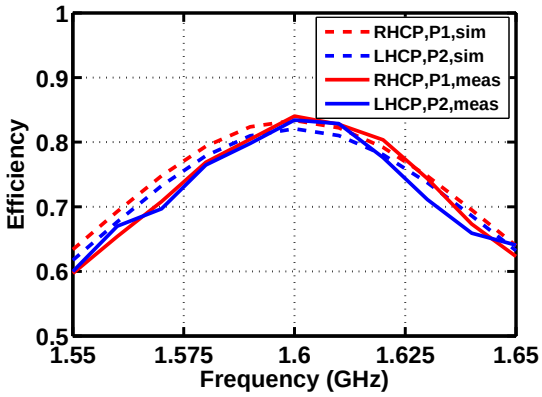

Fig. 9. Simulated and measured antenna efficiencies.

IV. Conclusion

A compact and robust dual CP patch antenna for combined Globalstar/GPS applications has been presented. The adoption of the high permittivity substrate instead of the air substrate greatly reduces the size of the antenna to $40 \times 40 \times 6$ mm^3, which is $0.21\lambda_0 \times 0.21\lambda_0 \times 0.03\lambda_0$ (λ_0 is the wavelength at 1570 MHz in free space), and provides extra robustness, making the antenna more sustainable and portable. To mitigate the bandwidth reduction due to the inclusion of the high permittivity substrate, a parasitic patch is utilized for enhancing the bandwidth. Dual CP is achieved with the help of the 90° hybrid. The designed antenna is validated by the measurement, showing a 5% fractional bandwidth (1570–1650 MHz) for both VSWR < 2, axial ratio (AR) less than 3 dB, and port isolation less than -6 dB.

References

[1] Y.-Q. Zhang, X. Li, L. Yang, and S.-X. Gong, "Dual-band circularly polarized annular-ring microstrip antenna for gnss applications," *IEEE Antennas Wireless Propag. Lett.*, vol. 12, pp. 615–618, Apr. 2013.

[2] Y. Gou, S. Yang, Q. Zhu, and Z. Nie, "A compact dual-polarized double e-shaped patch antenna with high isolation," *IEEE Trans. Antennas Propag.*, vol. 61, no. 8, pp. 4349–4353, Aug. 2013.

[3] M. Heckler, R. Farias, L. Pereira, E. Schlosser, and C. Lucatel, "Design of circularly polarized annular slot antennas for satellite navigation systems," in *Proc. 7th Eur. Conf. Antennas Propag. (EuCAP)*, Apr. 2013, pp. 361–365.

[4] Y.-X. Guo, L. Bian, and X. Q. Shi, "Broadband circularly polarized annular-ring microstrip antenna," *IEEE Trans. Antennas Propag.*, vol. 57, no. 8, pp. 2474–2477, Aug. 2009.

[5] S.-L. Yang and K.-M. Luk, "A wideband l-probes fed circularly-polarized reconfigurable microstrip patch antenna," *IEEE Trans. Antennas Propag.*, vol. 56, no. 2, pp. 581–584, Feb. 2008.

[6] O. Falade, Y. Gao, X. Chen, and C. Parini, "Stacked-patch dual-polarized antenna for triple-band handheld terminals," *IEEE Antennas Wireless Propag. Lett.*, vol. 12, pp. 202–205, Feb. 2013.

[7] Y. Li, Z. Zhang, Z. Li, J. Zheng, and Z. Feng, "High-permittivity substrate multiresonant antenna inside metallic cover of laptop computer," *IEEE Antennas Wireless Propag. Lett.*, vol. 10, pp. 1092–1095, Sep. 2011.

[8] D. Sievenpiper, D. Dawson, M. Jacob, T. Kanar, S. Kim, J. Long, and R. Quarfoth, "Experimental validation of performance limits and design guidelines for small antennas," *IEEE Trans. Antennas Propag.*, vol. 60, no. 1, pp. 8–19, Jan. 2012.

[9] C. A. Balanis, *Antenna Theory Analysis and Design*, 3rd ed. Hoboken, NJ: John Wiley and Sons, 2005.

[10] D. M. Pozar, *Microwave engineering*, 2nd ed. New York: John Wiley and Sons, 1998.